International Journal of Applied Research 2020; 6(10): 683-690

ISSN Print: 2394-7500
ISSN Online: 2394-5869
Impact Factor: 8.4
IJAR 2020; 6(10): 683-690
www.allresearchjournal.com
Received: 25-08-2020
Accepted: 29-09-2020

Dr. Bijendra Mohan
+2 BKD Zila School,
Darbhanga, Bihar, India

Corresponding Author:
Dr. Bijendra Mohan
+2 BKD Zila School,
Darbhanga, Bihar, India

Analysis of optical fiber mode

Dr. Bijendra Mohan

Abstract
This Paper has described how to compute the mode power distribution in step-index and parabolic-index fibres for any mode combination. It was shown that the entire leaky mode set of a graded-index fibre falls within the meridional numerical aperture for a graded-index fibre, and that leaky modes may cause distortion of the intensity profile. The use of the mode overlap integral to compute mode coupling between dissimilar fibres has been demonstrated and it was found that coupling efficiency between the modes in step and graded-index fibres of differing azimuthal mode number, was negligible. $LP_{2,1}$ Bessel Mode Laguerre-Gauss modes.

Keywords: optical, fibres, cladding, radial, azimuthal.

Introduction
This Paper present a derivation of the field solutions for multimode fibres, enabling any given modal distribution, and corresponding near-field intensity profile, to be computed. The categorization of LP modes into mode groups is described. The problem of avoiding the launch of leaky modes in graded-index fibres is highlighted and use of the mode overlap integral for computing coupling efficiency between fibres is demonstrated.

Step Index Fibre
Electromagnetic phenomena are governed by Maxwell's equation. These may be used to derive the Wave Equation, which describes the propagation of the electric field vector E in space and time [1], as follows:

$$\nabla^2 \bar{E} - \frac{\varepsilon_r}{c^2} \frac{\partial^2 \bar{E}}{\partial t^2} = 0 \quad (1.1)$$

where ∇^2 is the Laplacian operator, which in polar co-ordinates, is given by

$$\nabla^2 = \frac{\partial^2}{\partial r^2} + \frac{1}{r} \frac{\partial}{\partial r} + \frac{1}{r^2} \frac{\partial^2}{\partial \Phi^2} + \frac{\partial^2}{\partial z^2} \quad (1.2)$$

ε_r is relative permittivity and c is the velocity of light in a vacuum.

Fibre modes are solutions to the wave equation that satisfy certain boundary conditions and have a spatial distribution that does not change as it propagates. For simplicity it will be assumed that the fibre cladding extends to infinity. This assumption is valid because the power in the highest-order modes in both stepindex and graded-index fibres, with 50um core diameter, falls to a negligible value of less than 10^{-22} of its peak value at a radial distance of 62.5um, which is the typical cladding radius of the fibres used in this work.

Assuming separability, solutions for E, in polar co-ordinates, are of the form:

$$E(r, \Phi, z, t) = F(r) e^{j(\eta \Phi)} e^{j(\beta z - \omega t)} \quad (1.3)$$

Where:

$F(r)$ is a radial field function,
$e^{j(\eta \Phi)}$ is a periodic function,
η is the azimuthal mode number and takes integer values,
Φ is the azimuthal angle,
$e^{j(\beta z - \omega t)}$ is a periodic function of distance and time,

Substituting eqns. (1.3) and (1.2) into eqn. (1.1) gives

$$\frac{\partial^2 F}{\partial r^2} + \frac{1}{r}\frac{\partial F}{\partial r} - \frac{\eta^2}{r^2} F - \beta^2 F + \frac{\omega^2}{V^2} F = 0 \quad (1.4)$$

Rearranging gives

$$r^2 \frac{\partial^2 F}{\partial r^2} + r\frac{\partial F}{\partial r} + \left[r^2\left(n_{core}\, 2_{K_0{}^2} - \beta^2\right) - n^2\right]F = 0 \quad (1.5)$$

Which is Bessel's Equation, where K_O is the free-space wave number $(2\pi/\lambda)$ and n_{core} is the refractive index of the fibre core.

For a bound mode the propagation constant, b, takes values in the range

$$k_o n_{clad} \leq \beta \leq k_o n_{core} \quad (1.6)$$

Thus, in the core the inner bracket in eqn. (1.5) is positive giving a solution of the form

$$F(r) = J_\eta \left(r(n_{core}^2 k_o^2 - \beta^2)^{1/2}\right) \quad (1.7)$$

Where J_η is a Bessel function of order η. F(r) is thus aperiodic with core radius.

Similarly, in the cladding the inner term is negative and the solution is of the form

$$F(r) = K_\eta \left(r(\beta^2 - n_{clad}^2\, k_o^2)^{1/2}\right) \quad (1.8)$$

where K_η is a modified Bessel function of order η. F(r) is thus exponentially decaying in the cladding

Ignoring t and z in eqn. (1.3) the solution for the transverse component of the TE and TM fibre mode fields is

$$E(r, \Phi) = J_\eta \left(r(n_{core}^2\, k_o^2 - \beta^2)^{1/2}\right).e^{j(\eta\Phi)} \quad (1.9)$$

in the core, and

$$E(r, \Phi) = K_\eta \left(r(\beta^2 - n_{clad}^2\, k_o^2)^{1/2}\right).e^{j(\eta\Phi)} \quad (1.10)$$

in the cladding.

There is, however, a small field component in the forward, or z, direction which must be considered when calculating exact field solutions. This component leads to two further types of modes designated as EH and HE, depending on whether the electric or magnetic field is dominant in the z-direction. In a typical communications fibre, however, the index difference between the core and the cladding is very small, leading to only glancing angles at the core/cladding interface. The transverse, TE and TM, components thus dominate and certain groupings of TE, TM, HE and EH modes have almost identical propagation constants enabling them to be combined into Linearly Polarised, or LP, modes [2]. The LP approximation thus enables the fibre modes to be fully described by eqns. (3.9) and (3.10).

In order to calculate the mode fields it is necessary to determine the values of b. This may be achieved by matching the tangential field components at the core/cladding interface, resulting in the following expression:

$$U\frac{J_{\eta\pm1}(U)}{J_\eta(U)} = \pm W \frac{K_{\eta\pm1}(W)}{K_\eta(W)} \quad (1.11)$$

Where

$$U = a(n_{core}^2\, k_o^2 - \beta^2)^{1/2} \quad (1.12)$$

and

$$W = a(\beta^2 - n_{clad}^2\, k_o^2)^{1/2} \quad (1.13)$$

As an example, a plot of the terms in eqn. (1.11), for a 50um core diameter fibre with 0.21NA at 850nm, is shown in Figure 1.1, where a value of η = 4 has been used. The required values of β correspond to the crossing points of the two sets of curves, for the left and right sides of eqn. (1.11). In this example, there are 11 modes for this particular azimuthal mode number.

Each discrete mode, with the same η value, is designated by its radial mode number, where $\mu = 1$ corresponds to the mode at the right end of the plot with the highest value of β and $\mu = 11$ corresponds to the mode nearest cut-off.

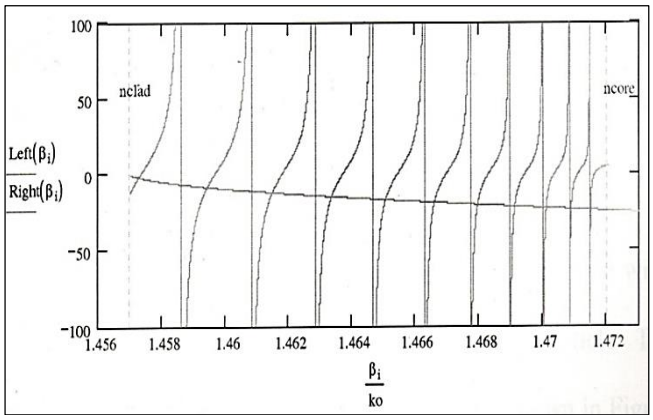

Fig 1: Matching tangential fields at core/cladding interface to determine propagation constants in a step-index fibre

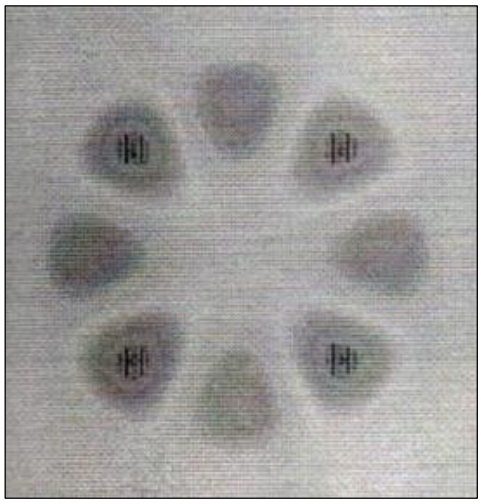

μ = 1

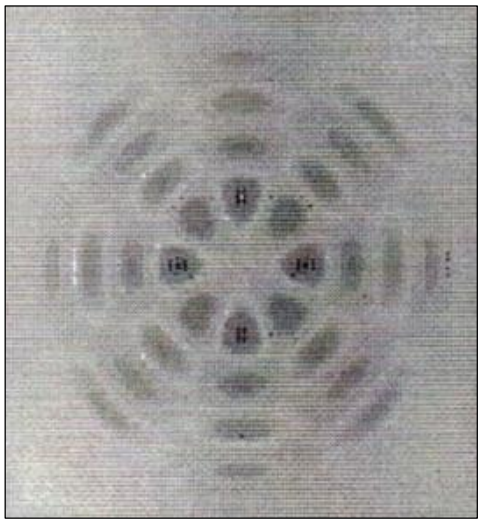

μ = 4

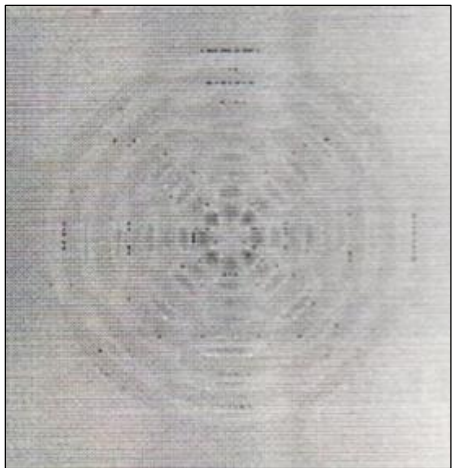

$\mu = 11$

Fig 2: Examples of field distributions for modes in step index fibre having azimuthal mode number $\mu = 4$ and different radial mode numbers, μ

Mathcad software [3] was then used to compute the mode fields and some examples for $\eta = 4$ are given in Figure 1.2, where red is positive and blue is negative field values.
The mode pattern that would be observable with, for example, a camera, is given by the square of the field. The corresponding power plots for the modes above are shown in Figure 1.3.

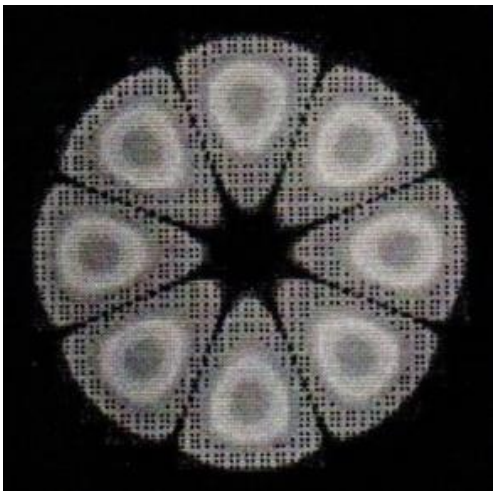

$\mu = 1$

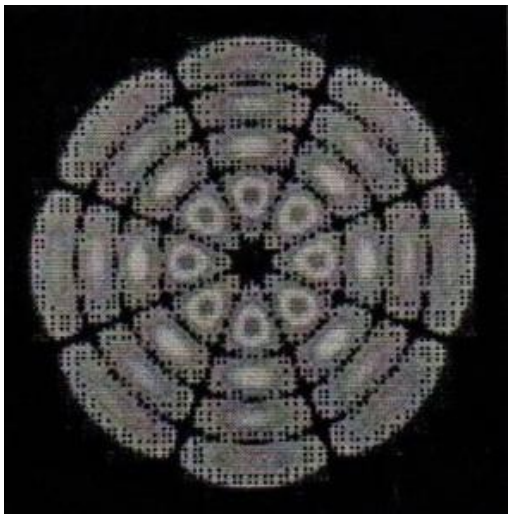

$\mu = 4$

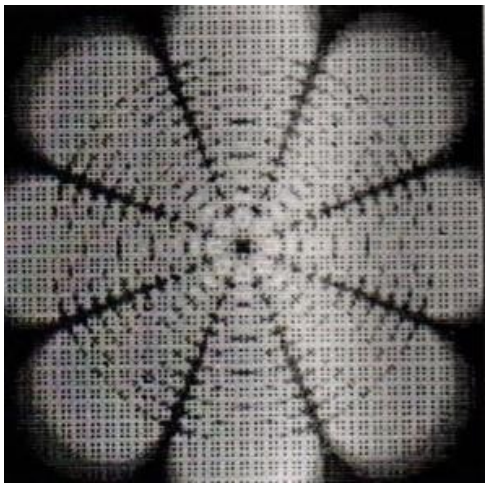

Fig 4: Examples of power distributions for modes in step index fibre having azimuthal mode number $\eta = 4$ and different radial mode numbers, μ

The standard designation for the LP modes shown here is $LP_{\eta,\mu}$. It can be seen that m gives the number of intensity maxima in the radial direction and 2η gives the number of intensity maxima in the azimuthal direction.
It can be seen from the exponential terms in eqns. (1.9) and (1.10) that the azimuthal dependence can be either cos (ηΦ) or sin (ηΦ), subject to arbitrary phase. The effect of this is give two degenerate modes for each β value, which are rotated slightly with respect to each other. An example in shown in Figure 1.4, below, for the two degenerate $LP_{3,2}$ modes.

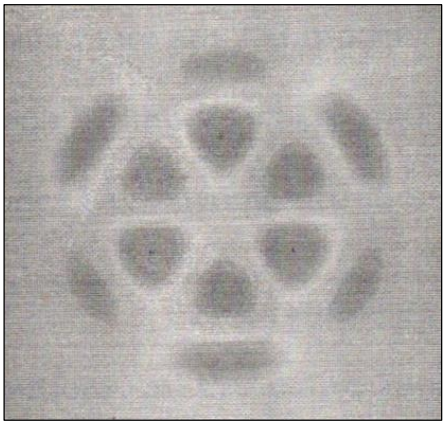

$\mu = 2$

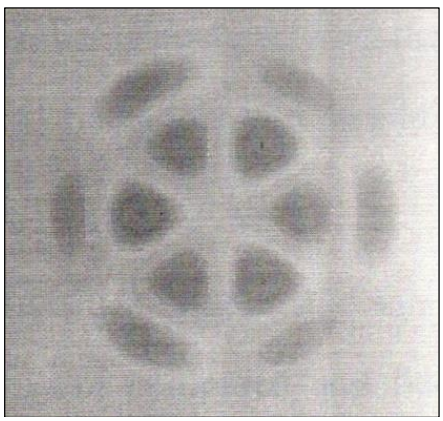

$\eta = \mathbf{3}$

Fig 4: Field plots of two degenerate forms of $LP_{3,2}$ mode in step-index fibre

Modal Excitation of Step-Index Fibre

The number of modes, N, in a step-index fibre is given approximately by [2]

$$N = \frac{V^2}{2} \quad (1.14)$$

Where V is the normalised frequency, given by:

$$V = ak_oNA \quad (1.15)$$

and a is the core radius, NA is the fibre numerical aperture, given by,

$$NA = n_{core}\sqrt{2\Delta} \quad (1.16)$$

and D is the relative index difference of the fibre, given by,

$$\Delta = \frac{n_{core}^2 - n_{clad}^2}{2n_{core}^2} \quad (1.17)$$

For example, for a 50um step-index fibre, 0.21NA at 850nm there are 753 modes. This number is made up from the fact that each LP mode, where $\eta \neq 0$ has two orientations and in addition, all modes lave two polarisation states.

To simulate a fully-filled fibre, the intensity distribution of the entire mode set were computed and linearly combined. The normalised intensity distribution and a profile through its centre, are shown in Figure 1.5. It can be seen that the intensity profile is a similar same shape to the step-index profile, as expected.

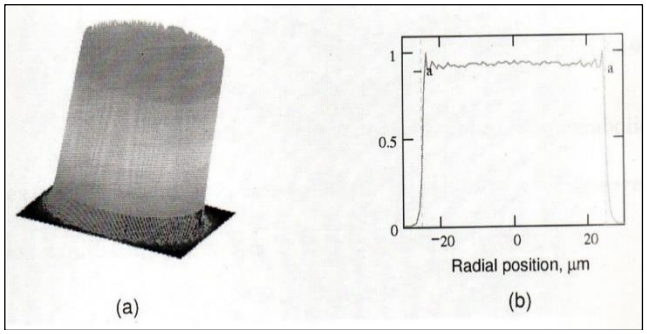

Fig 5: Power distribution of all guided modes, equally weighted, in 50 um core diameter step-index fibre. (a) 3-D model, (b) intensity profile.

Graded-Index Fibre

Consider a power-law index profile, n(r), given by,

$$\text{n(r)} = n_{core}\left[1 - 2\Delta\left(\frac{r}{a}\right)^{\alpha}\right]^{0.5} \left(\frac{r}{a}\right) \leq 1 \quad (1.18)$$

where a is the profile factor.

Substituting eqn. (1.18) into eqn. (1.5) gives,

$$r^2\frac{\partial^2 F}{\partial r^2} + r\frac{\partial F}{\partial r} + [r^2(n(r)^2k_o^2 - \beta^2) - \eta^2]F = 0 \quad (1.19)$$

This is the *Helmholtz equation* and, for a parabolic index profile where a = 2, has solutions in the form of Laguerre-Gauss modes [4], as follows

$$E_{\eta,\mu}(\rho, \Phi, Z) = \rho^{\eta}e^{\frac{-\rho^2}{2}}L_{\mu-1}^{\eta}(\rho^2)\sin(\eta\Phi + \theta_o)e^{-j(\beta z)} \quad (1.20)$$

where the radial variable is given by

$$\rho = \frac{r}{a}\sqrt{V} \quad (1.21)$$

and

$$L_{\mu'}^{\eta}(\rho^2)\sum_{s=0}^{\mu'}\frac{(\mu'+\eta)!(-1)^s\rho^{2s}}{(\eta+s)!\,(\mu'-s)!s!} \quad (1.22)$$

is the generalised Laguerre polynomial, where, for convenience, the substitution $\mu' = \mu - 1$ has been made. $\theta_o = 0\ or\ {}^{\pi}/_{2,}$ represents pairs of degenerate modes when $\eta \neq 0$.

Some typical field plots for a 50um, 0.21NA fibre at 850nm are shown in Figure 1.6 and the corresponding intensity distributions are shown in Figure 1.7.

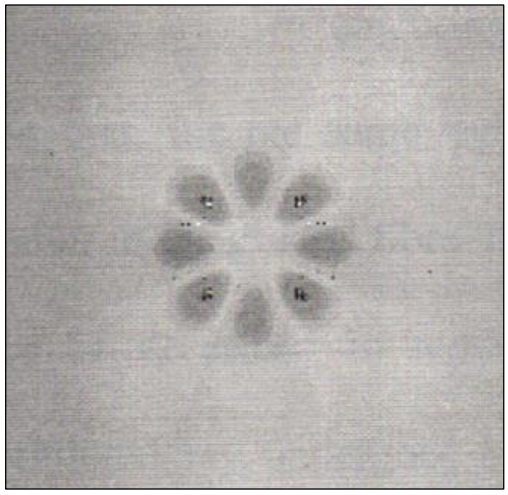

$\mu = 1, \eta = 4$

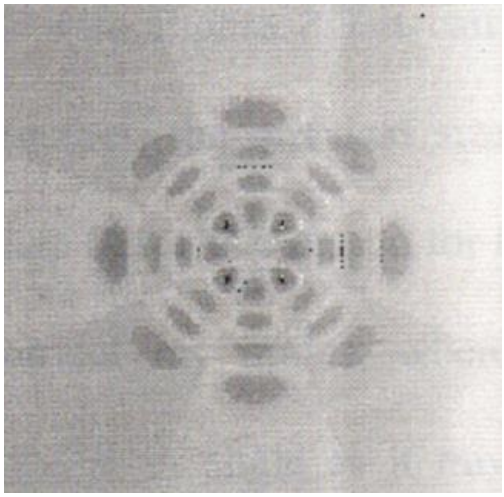

$\mu = 4, \eta = 4$

Fig 6: Examples of field distributions for modes in parabolic-index fibre having azimuthal mode number $\eta = 4$ and different radial mode numbers, μ

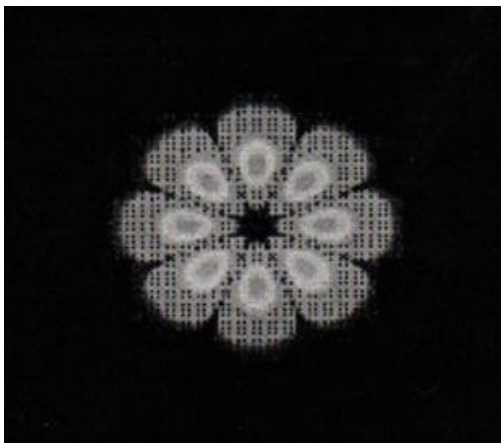

$\mu = 1, \eta = 4$

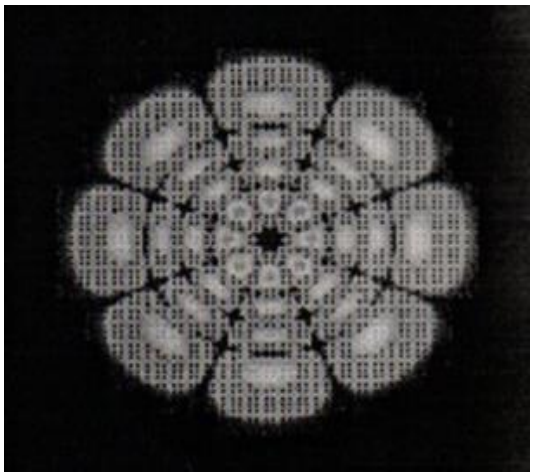

$\mu = 4, \eta = 4$

Fig 7: Examples of power distributions for modes in parabolic-index fibre having azimuthal mode number $\eta = 4$ and different radial mode numbers, μ

Comparing Figure 1.7 with Figure 1.3 it can be seen that, for the same radial mode number, the physical size is smaller in the graded fibre than for the step fibre. The reason for this may be described in terms of geometrical ray optics, where a meridional ray undergoes a constant change in angle as it travels radially out form the centre. Now for a particular ray the propagation constant, β, defined as

$$\beta = k_o n(r)\cos(\theta) \qquad (1.23)$$

is invariant. Thus, as a ray enters a region of lower refractive index, towards the cladding boundary, from eqn. (1.23), θ decreases accordingly and eventually turns back towards the core centre. The higher-order mode, therefore, occupies a physically greater proportion of the core diameter than a lower-order mode.

Modal Excitation of Graded-Index Fibre

The number of modes, N, in a graded-index fibre is given approximately by

$$N = V^2 \left[\frac{\alpha}{2(\alpha+2)}\right] \qquad (1.24)$$

As an example, in a 50mm graded-index fibre, 0.21NA at 850nm there are about 276 modes.

Figure 1.8 shows a linear combination of the entire mode set for a parabolic index fibre. The intensity profile is a similar shape to the parabolic index profile.

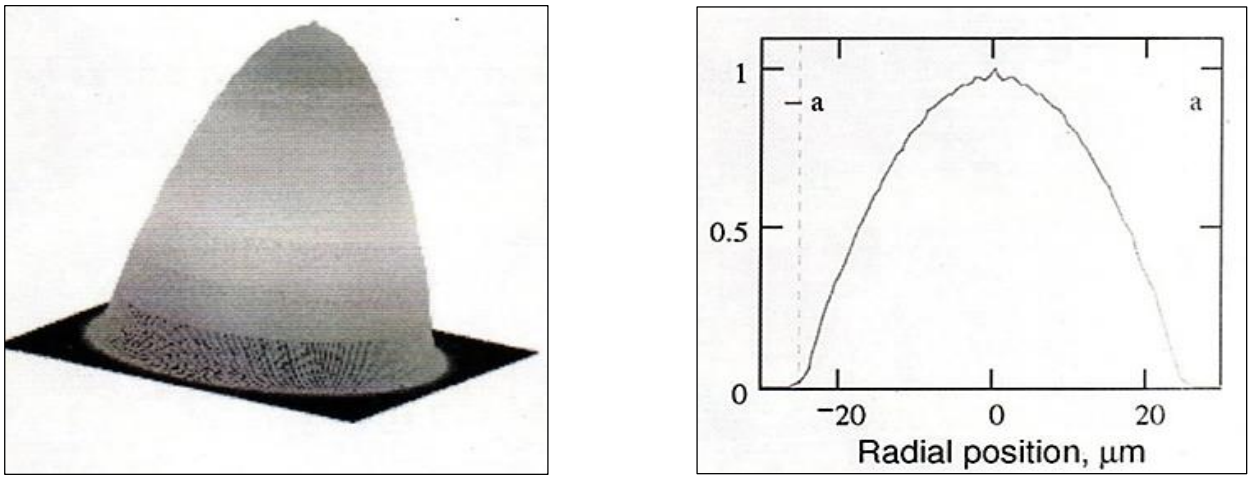

(a) (b)

Fig 8: Power distribution of all possible guided modes, equally weighted, in 50um core diameter parabolic index fibre, (a) 3-D model, (b) intensity profile

Mode Groups

Using the WKB approximation [4] the propagation constant of a mode in a graded-index is given by [5]

$$\beta = k_o n_{core}\left(1 - 2\Delta\left(\frac{m}{M}\right)^{2\alpha/(2+\alpha)}\right)^{1/2} \qquad (1.25)$$

where m is the Principal Mode Number, defined as

$$m = 2\mu + \eta - 1 \qquad (1.26)$$

and M is the maximum principal mode number, given by

$$M = \sqrt{\frac{\alpha}{\alpha+2}} k_o n_{core} a\sqrt{\Delta} \qquad (1.27)$$

From eqn. (1.26) there are several combinations of (η, μ) that have the same principal mode number and are therefore degenerate. For example, in a parabolic index fibre with 50um core diameter and 0.21 NA, there are, from eqn. (1.27) 19 mode groups at 850nm.

It should be noted, however, that Finite Element methods [6] show that propagation constant of modes within in the same mode group typically differ from each other by about 0.0007%. This is much smaller than the difference in propagation constant between adjacent mode groups, typically 0.055%, and so is negligible for most purposes.

The number of individual modes in each mode group is equal to twice the mode group number. For example, in mode group m = 5 the possible combinations of (η, μ) are $LP_{4,1}$, $LP_{2.2}$ and $LP_{0,3}$. Now, as described in section 1.1.1, there are two field orientations for modes when $\eta \neq 0$, and two polarisation states for each mode, making a total of ten modes in this group.

The $LP_{\eta,\mu}$ modes of the first 16 mode groups in a 50um core diameter graded index fibre, at 850nm, are shown in Figure 1.9.

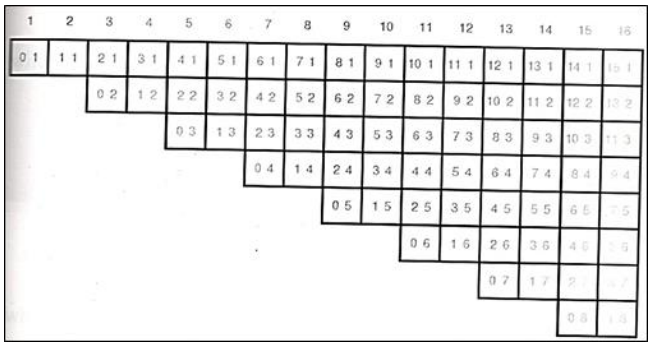

Fig 9: Tabulation of the first 16 mode groups in a 50um graded-index fibre at 850nm. Mode group numbers in blue and $LP_{\eta,\mu}$ designation in green

Assuming all modes are equally excited, the near-field intensity distribution P_g of each mode group m is given by

$$P_g(m)\sum_{\mu=1}^{int[(m+1)/2]}\left[\left(E_{\eta,\mu}\right)^{+2}_{\theta_o=0}+\left(E_{\eta,\mu}\right)^{2}_{\theta_o=\pi/2}\right] \quad (1.28)$$

where, from eqn. (1.26), $\eta = m + 1 - 2\mu$.

The total near-field distribution P_{tot} is given by

$$P_{tot} = \sum_{m=1}^{M}\left[P_g(m).MTF(m)\right] \quad (1.29)$$

where, for a fully-filled fibre, MTF(m) = 1 for all mode numbers.

Examples of near-field profiles for mode group numbers 4 and 14 are shown in Figure 1.10 where it can be seen that the power distributions consist of circularly symmetric rings where the number of rings corresponds to half the mode group number.

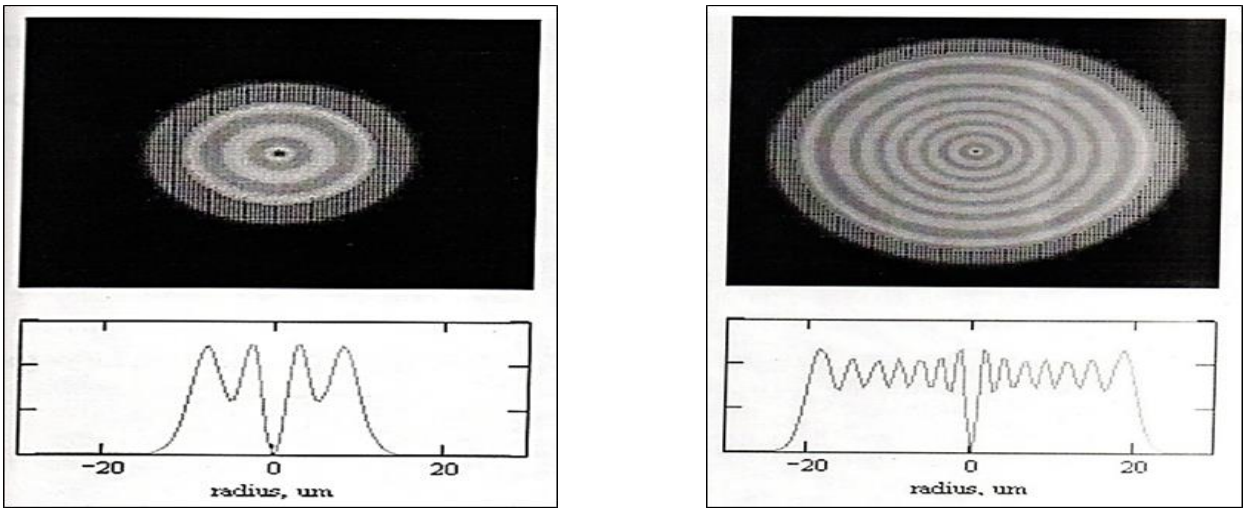

Mode group 4 Mode group 14

Fig 10: Intensity distributions of mode group numbers 4 and 10 in a 50um graded-index fibre.

1.2.3 Leaky modes

In the guided mode regime where

$$k_o n_{clad} \le \beta \le k_o n_{core} \quad (1.30)$$

modes exist within two caustics, defined by positive values of the coefficient of F(r) in the Helmholtz equation, eqn. (1.19), as follows,

$$(n(r)^2 k_o^2 - \beta^2) - \left(\frac{\eta^2}{r^2}\right) \ge 0 \quad (1.31)$$

There exists, however, a region where the mode is beyond cut-off, but satisfies the following inequality [7]:

$$k_o^2 n_{clad}^2 - \frac{\eta^2}{a^2} \le \beta^2 < k_o^2 n_{clad}^2 \quad (1.32)$$

This situation is represented in Figure 1.11, where the $LP_{16,3}$ mode, for example, is bound in the region 11 um to 24 um and is radiative beyond 32um. From a quantum-mechanical point of view, the guided light can be described as tunnelling through part of the cladding, via the evanescent tail, and then coupling to a radiation mode. Some leaky modes are rapidly attenuated after a few cm where as other may propagate for a km or more [8].

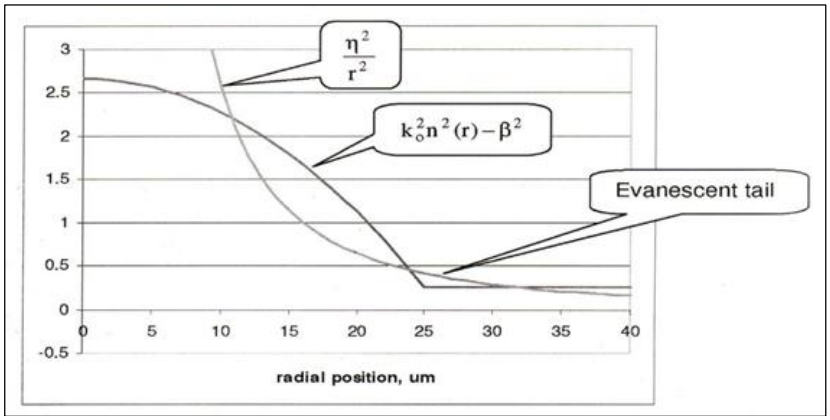

Fig 11: Plot of terms in eqn. (1.31) showing a leaky mode, $LP_{16,3}$

In a graded-index fibre the total number of leaky modes is given by,

$$N_{leaky} = \frac{V^2}{12} \quad (1.33)$$

where:

$$V = k_o aNA \quad (1.34)$$

Comparison with eqn. (1.24) indicates that leaky modes can carry up to 25% of the total power in a graded-index fibre.
The field distribution of leaky modes can also be calculated using eqn. (1.20), where the (h, m) values of leaky modes must satisfy the following inequality [8],

$$M \leq 2\mu + \eta - 1 \leq M + \frac{\eta^2}{4M} \quad (1.35)$$

where M is the number of guided mode groups, given by eqn. (1.27)
As an example, in a 50um fibre at 850nm there are 120 leaky modes, including both polarisations and azimuthal orientations, making a total of 30 discrete (η, μ) combinations.
The effect of leaky modes in to distort the near-field intensity distribution. This can be seen in Figure 1.12 where the complete leaky mode spectrum has been added to the guided mode spectrum, shown in blue. The intensity profile is much squarer than the quasi-parabolic shape of the guided modes alone.
The presence of leaky modes has long been a source of difficulty for refractive index profiling methods that are based on the principle that the shape of the index profile is approximately proportional to the intensity profile if all the guided modes are equally excited. The presence of leaky modes seriously perturbs the accuracy of these methods and several efforts have been made to compensate from them [9].
Leaky modes are difficult to avoid as they lie entirely within the meridional NA of a fibre. The impact of leaky modes in mode control devices will be discussed in PAPER 6.

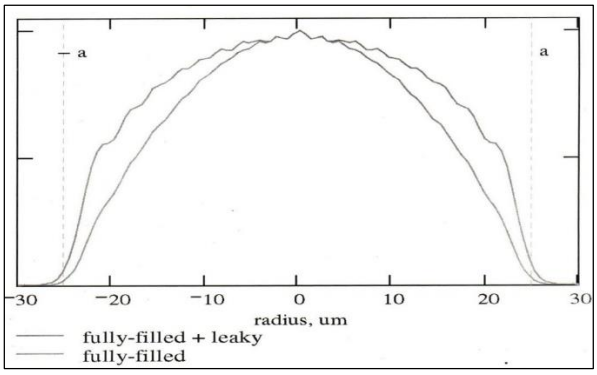

Fig 12: Computed near-field intensity profile of 50um graded-index fibre showing guided modes (red) and effect of adding leaky modes to guided modes (blue)

Mode Overlap Integral

To determine the mode distribution coupled into a target fibre from a source fibre it is necessary to compute the mode overlap factor ε of each source mode E_s with each target mode E_T. The overlap integral required to do this is as follows,

$$\varepsilon = \frac{\iint E_S(x,y)E_T(x,y)dxdy}{\sqrt{\iint E_S(x,y)E_S(x,y)dxdy}\sqrt{\iint E_T(x,y)E_T(x,y)dxdy}} \quad (1.36)$$

The mode overlap factor can take values from zero, in the case of no overlap, for example belonging to the same waveguide, to unity, for complete overlap.
The overlap integral has to be evaluated numerically for each mode combination and is therefore computationally intensive. It was found, however, that for Bessel and Laguerre-Gauss (LG) modes e was negligibly small for coupling between modes of a different azimuthal mode number η. Thus, it was only necessary to compute e for modes having the same value of η.
As an example, Table 1.1 shows $|\varepsilon|$ values for coupling between the $LP_{2,1}$ Bessel mode and the $LP_{2,\mu}$ LG modes. Note that the sum of the squares of the coefficients in the Table is close to unity, indicating that power coupled into modes with a different azimuthal mode number is very small.

Table 1: Overlap coefficients between $LP_{2,1}$ Bessel mode and $LP_{2,\mu}$ Laguerre-Gaussian modes

$LP_{2,1}$	$LP_{2,2}$	$LP_{2,3}$	$LP_{2,4}$	$LP_{2,5}$	$LP_{2,6}$	$LP_{2,7}$	$LP_{2,8}$	$LP_{2,9}$
0.305	0.414	0.451	0.437	0.389	0.319	0.238	0.154	0.077

To compute the near-field power distribution coupled into the graded fibre for the $LP_{2,1}$ mode in the example above, the power distributions of the modes shown in Table 1.1 were added in proportion to the square of the value of their respective overlap coefficients. Figure 1.13 shows the power distribution of the $LP_{2,1}$ Bessel mode and the resultant power distribution coupled into a graded-index fibre. It can be seen that the latter has the same four-lobed shape as the $LP_{2,1}$ Bessel mode but that power is distributed over a range of radial mode numbers μ.

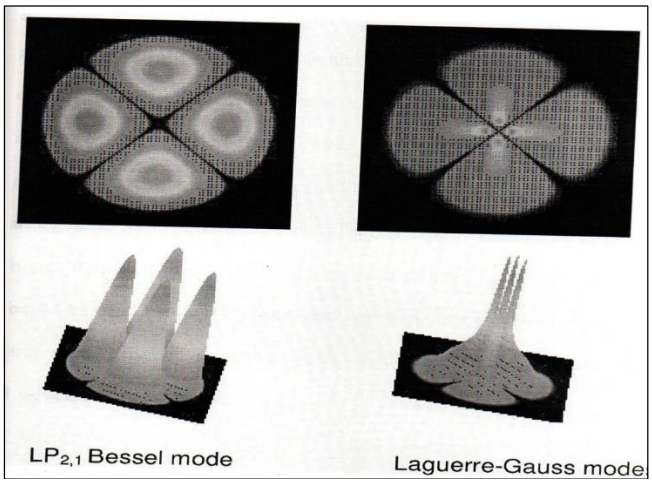

Fig 13: Mode power distributions for the $LP_{2,1}$ Bessel mode in a step-index fibre and for the power distribution coupled into a graded-index fibre

References

1. Senior JM. "Optical Fibre Communications", section 2.3, Prentice Hall, second edition 1992.
2. Golge D. 'Weakly Guiding Fibres', Appl. Opt 1971;10(10):2252-2258.
3. http:/www.mathsoft.com
4. Berdague S, Facq P. 'Mode division multiplexing in optical fibres', Appl. Opt 1982;21(11):1950-1955.
5. Gloge D, Marcatili EAJ. 'Impulse response of fibres with ring-shaped parabolic index distribution', Bell Syst. Teach. J 1973;52(7):1161-1168.

6. Liu Y *et al*. 'Accurate mode characterization of the graded-index multimode fibres for the application of mode-noise analysis', Appl. Opt 1995;34(9):1540-543.
7. Adams MJ *et al*. 'Leaky rays on optical fibres of arbitrary (circularly symmetric) index profiles', Electron. Lett 1975;11(11):238-240.
8. Olshansky R. 'Leaky modes in graded index optical fibres', Appl. Opt 1976;15(11):2773-2777.
9. Sladen F *et al*. 'Determination of optical fibre refractive index profiles by a near-field scanning technique', Appl. Phys. Lett 1976;28(8):225-258.